Development and Analysis of Trapped Field Magnets in Electromechanical Devices

Kent R. Davey, *Fellow, IEEE*, Roy Weinstein, and Ravi Sawh

***Abstract* — High temperature superconducting trapped field magnets (TFM) offer great potential as an alternative to 2nd generation YBCO wire, both in cost and performance. Attention is given to the calculation of current distribution within YBCO disks at partial and full activation and comparing this to experimental values. The best results are obtained by treating the current as a sequence of nested current rings. The fields are computed by integrating the elliptic integrals representing the fields from these rings and using variable metric optimization to choose the ring radii to best match the activation field over the un-activated material. A technique for treating the sub-regions of the TFM as voltage fed coils appears most expeditious for computing forces.**

***Index Terms*—activation, bulk, HTS superconductor, variable metric optimization, synchronous motors**

I. Introduction

BULK HTS SUPERCONDUCTORS can trap fields of 10.1 T before cracking under magnetic pressure, and with special provisions, fields of 14 and 18T have been demonstrated [1][2]. Crapo and Weinstein previously showed that pulsed activated TFMs could be used on motors and generators [3]. There is great difficulty in controlling the crystalline growth to form single grains. The performance of larger bulk materials with multiple sub-domains is usually quite poor. Preliminary work has been directed to assemble these smaller pucks into arrays. Multiple layers are required to compensate for zero normal current boundaries [4].

Effectively integrating bulk trapped field magnets into electromechanical devices is proving to be a challenge. The simplest application is that of magnetic bearings where the induced currents within the bulk YBCO produce stable repulsive forces against conventional permanent magnets in the rotating member [5]. Qiu [6] has successfully used the material in a reluctance machine to enhance saliency. The material is operated zero field cooled. Matsuzaki's group has developed an axial flux bulk HTS synchronous machine in which the pucks are pulse activated to a field level of 0.35 to 1 T max [7]. Specially processed YBCO pucks are capable of sustaining 2.1 T at 77 K; the challenge will be to activate arrays of these pucks in situ.

It is essential to know the distribution of the current to design electromechanical devices with this material. Palka attempts an inverse problem calculation of these currents based on external field measurements [8]. An iterative process is employed in which the magnetic flux and the current density become degrees of freedom adjusted to avoid a variation of magnetic flux within the material [9]. An average "engineering" current density is assigned to different subregions in an effort to minimize the least squares fit to measured magnetic field data external to the bulk material.

In the section that follows, the current density is determined by integrating elliptic integrals through the bulk material and using a variable metric optimization routine [10] to find the distribution.

II. Getting the Currents and the Forces

Critical current density J_c is directly correlated to temperature within these magnetic field bounds. If the material becomes superconducting at temperature T_c, and the current density is known to be J_1 at temperature T_1, then the current density at temperature T_2 will be

$$J_c(T_2) \approx J_c(T_1)\left(\frac{(T_c - T_2)}{(T_c - T_1)}\right)^2 \qquad (1)$$

The current density distribution is unknown. How this current density distribution is computed is best explained through the following example.

Suppose a YBCO puck is exposed to a magnetic field (applied parallel to the c-axis) equal to or greater than the largest B field that can be supported by a current density of J_c throughout the puck. For YBCO prepared using the U/n method, this value is 2.1 T. If the material is exposed to this field, cooled, and then the source field removed, a current density of J_c will reside in the puck. It is in a state of full activation. A current density of the same value J_c resides in the puck when it is exposed to a 1T field during activation, but the only a portion of the puck will have current, and the remainder will have none.

Smythe[11] shows that the field of a circular current loop with radius a and current I at location ρ,z is

$$B_\rho = \frac{\mu I}{2\pi}\frac{z}{\rho\sqrt{(a+\rho)^2+z^2}}\left[-K + \frac{a^2+\rho^2+z^2}{(a-\rho)^2+z^2}E\right] \qquad (2)$$

Manuscript received August 10, 2006.

Kent Davey is with the Center for Electromechanics, University of Texas, 10100 Burnet Rd., Bldg. EME 133, Austin, TX 78758, USA (phone: 512-232-1603; fax: 512-475-7700; e-mail: k.davey@mail.utexas.edu).

Roy Weinstein and Ravi Sawh are with the Beam Particle Dynamics Laboratories, University of Houston, 632 Science & Research Bldg 1, Houston, TX 77204-5005, USA (Weinstein@uh.edu).

$$B_z = \frac{\mu I}{2\pi}\frac{1}{\rho\sqrt{(a+\rho)^2+z^2}}\left[K+\frac{a^2-\rho^2-z^2}{(a-\rho)^2+z^2}E\right] \quad (3)$$

where K and E are complete elliptic integrals of the first and second kind, each evaluated at the argument

$$k=\sqrt{\frac{4a\rho}{(a+\rho)^2+z^2}}. \quad (4)$$

The fields for a disk with finite thickness and height are obtained by numerically integrating (2) and (3), here with a 48 point Gauss Legendre integration [12]. For each disk spanning a radius from r_1 to r_2, and height z_1 to z_2 the ρ directed field is

$$B_\rho = \int_{z_1}^{z_2}\int_{r_1}^{r_2} B_{\rho_{ring}}(r,z)\,dz\,d\rho = \frac{(r_2-r_1)(z_2-z_1)}{4}\sum_{k=1}^{48}\sum_{i=1}^{48} w_k w_i B_\rho(r_i,z_i) \quad (5)$$

where

$$r_i=\frac{r_2+r_1}{2}+\left(\frac{r_2-r_1}{2}\right)x_i,\quad z_i=\frac{z_2+z_1}{2}+\left(\frac{z_2-z_1}{2}\right)x_i$$

A similar expression holds for B_z; the weights x_i and w_i are listed in [12].

When a puck is partially activated with a field B_a smaller than the critical field commensurate with J_c, the center of the puck will have no current density. The bulk material will have current at density J_c in such a distribution as to reproduce a homogeneous field of value B_a through as much of the central region as possible. For a vertical activation field, only ¼ of the problem need be modeled. The objective is to homogenize the field at level B_a in the rain drop shaded region of Fig. 1.

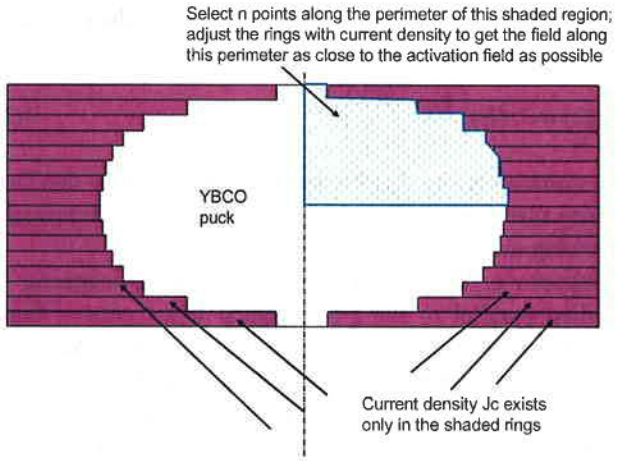

Fig. 1 In a partially activated puck, current density exists only on the periphery of the puck.

The uniqueness theorem shows that this objective is achieved if the field around the perimeter of that same region is made equal to B_a. The problem becomes an unconstrained optimization to determine the minimum radius of each of n rings to minimize the difference of the analytical field from the target field B_a at n points on the perimeter of the shaded region in terms of the field due to the various rings B_{ring},

$$\Im = \sum_{i=1}^{n}\left(\sum_{k=1}^{m} B_{ring\,k}(r_i,z_i) - B_a\right)^2 \quad (6)$$

A variable metric optimization produces the current density distribution shown for upper right quadrant for a 2 step, 3 step, 8 step, and a continuous distribution representation in Fig. 2. The current crowds towards the faces normal to the impressed activation field. It is impractical to work through this exercise for very large problems. Fortunately, it is usually unnecessary. The simple two step current density pattern representation experiences a force of 82.1 N when placed in a 1 T external field. By contrast, the smooth model accurate to better than 0.7% experiences a force of 80.7 N. The simplest 2 step approximation differs from the most accurate by only ~ 2% in force.

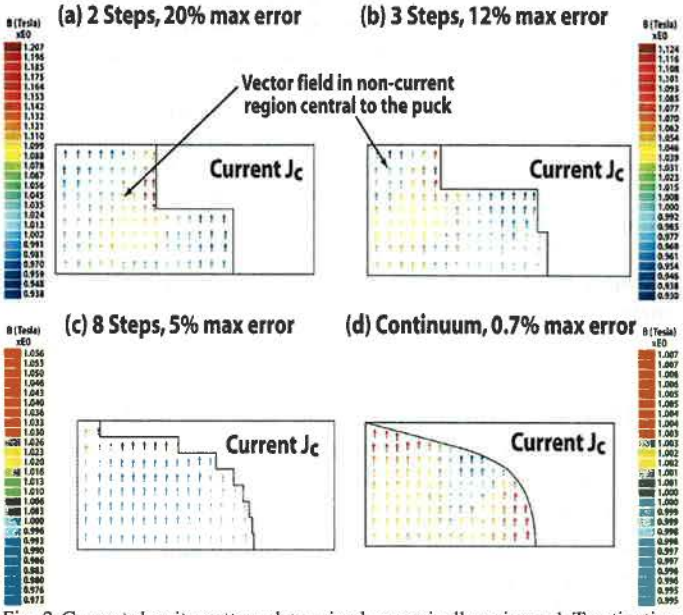

Fig. 2 Current density pattern determined numerically using a 1 T activation field and J_c=400 MA/m^2.

This process is tedious and time consuming. A more streamlined approach is to treat the puck as a set of nested voltage fed coils. If the resistance of the coil is zero, then the voltage dictates the flux. The voltage of a set of nested coils can be carefully chosen by pre-calculation to match the flux penetrating the puck before cooling. The current density in the coils must be checked to ensure none exceed J_c.

III. Comparing Experiment to Theory

A 20 mm diameter YBCO TFM disk, 8 mm high was activated at three different field levels, ~ 2.1 T, ~ 0.7 T, and ~ 0.35 T. The first activation level, 2.1 T, is used to fully activate this puck. The vertical field is measured 0.7 mm just above the top surface of the TFM puck. The steps required for the field theoretician to predict this field are as follows:

1. Assume a homogeneous azimuthally directed volume current in the puck and back calculate the magnitude required to produce the maximum field supported at the surface on the axis. For this geometry and 2.1 T, $J_c = 4\cdot10^8$ A/m^2.

2. Break the puck into sub-regions; define each sub region as a one turn voltage excited coil with zero resistance and zero external reactance.
3. Frequency can be set to anything convenient (60 Hz). Compute the voltage induced in each sub-region coil when the puck is placed in an impressed homogeneous vertical field of 0.35 T, 0.7 T, and 2.1 T.
4. Assign each of the sub-region coils the voltage computed in step 3 (angle of 90°). Compute the field everywhere with the impressed field off and along with that field the current induced in each of the sub-region coils. Each sub-region coil current is inductance limited only, so that the flux linking each coil is $V/(j\omega)$.
5. For every sub-region that has a current density exceeding Jc, replace that voltage fed coil with a volume current with density $Jc<0$.
6. Repeats steps 4 and 5 until no currents induced in a voltage induced coil exceed the current density Jc. Several iterations are required typically.

The measured and computed B field for each of the three activations cited above is shown in Fig. 3. The measurements are taken about 5.5 hours after activation.

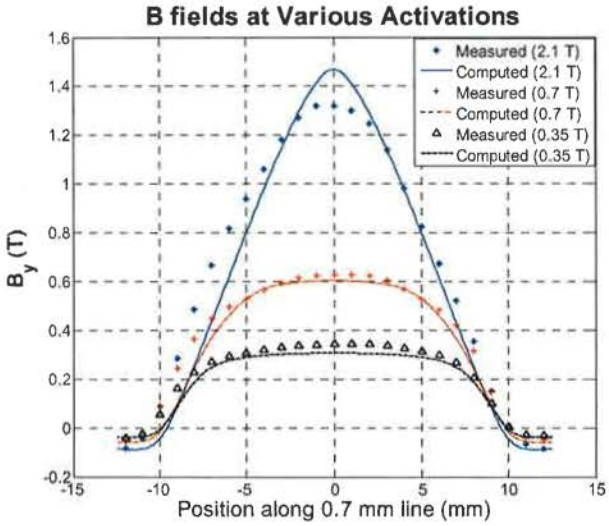

Fig. 3 Comparison of magnetic fields computed for 2.1 T, 0.7 T, and 0.35 T activation. All fields are measured 0.7 mm above the surface of the puck.

IV. Reasons for Errors in this Model

The TFM pucks tested are real non ideal crystals; this is the reason for the small asymmetry of the fields recorded. Two additional phenomena complicate the modeling of TFM's, creep and J_c dependence on B. Creep is easier to deal with.
Until recently, it was thought that natural field decay within a TFM would prohibit its usefulness in practical applications. For the melt textured YBCO materials discussed in this paper, the decay is 4-5% per decade of time. For example, if B initial is 1 T ten minutes after activation, it will be 0.96 T G at 100 minutes, 0.921T at 1000 minutes, 0.884T at 10,000 minutes, 0.849 T at 100,000 minutes, 0.814 T at 1,000,000 minutes (2 years) and 0.782 T at 10,000,000 minutes (20 years). Thus, field loss is limited to ~20% and becomes more stable with elapsed time. Furthermore, a simple procedure involving a small degree of cooling after activation has been developed to reduce creep to essentially zero.

Without the subsequent cooling, the field will have the time dependence shown in Fig. 4. Creep is related to activation level. Activation close to the maximum supported field will be characterized by a 2% creep loss in 5.5 hours. By contrast, a lower field activation registers close to 0.1% creep in the same time. The data perturbation witnessed from 180 to 210 minutes for each of the three curves is due to thermal variations brought on by the addition of liquid N_2. The apparent rise in the 0.7 T measurement is an artifact caused by the addition of the liquid coolant after 1 hour.

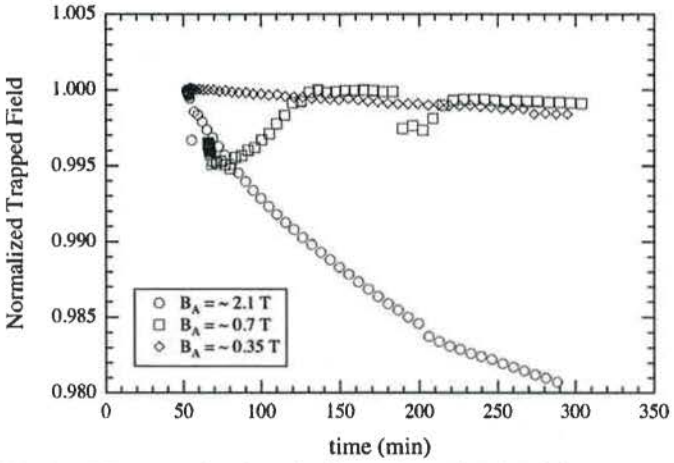

Fig. 4 B Field measured on the axis of the puck as a function of time.

Note that the shoulders of the computed fields fall off sooner than does the measured data. The TFM model followed thus far assumes the current density at peak activation is constant through the volume, the so called Bean's model [13]. The Kim-Bean model [14] is more accurate and accounts for the fact that J_c is higher were B is lower. Weinstein previously proposed another field model that supplements volume current with surface current [15]. When the B field decreases, Jc increases [16].

V. Forces on Zero Field Cooled TFM's

A first step in computing forces on zero field cooled TFM's is to assign a zero voltage condition. This remains a good approximation assuming the induced current density remains below J_c. The material used for this experiment is supplied by Can Superconductor, (http://www.can.cz/levitdisks.php), and the material specifications are supplied at their web site. The trapped fields as a function of temperature are supplied for their 21 mm diameter puck. A 0.7 T field is listed at 77 °K. A current density of $2.19 \cdot 10^8$ A/m^2 generates the field recorded 1.5 mm above the puck interface.
A 0.5 T NdFeB permanent magnet with a 15 mm diameter and height is moved from the surface of the TFM to a height of 5 mm and the repulsive force is measured as a function of height. Fig. 5 shows what the vector B field looks like as the

current density in the TFM builds from the outer radius in to minimize flux linkage.

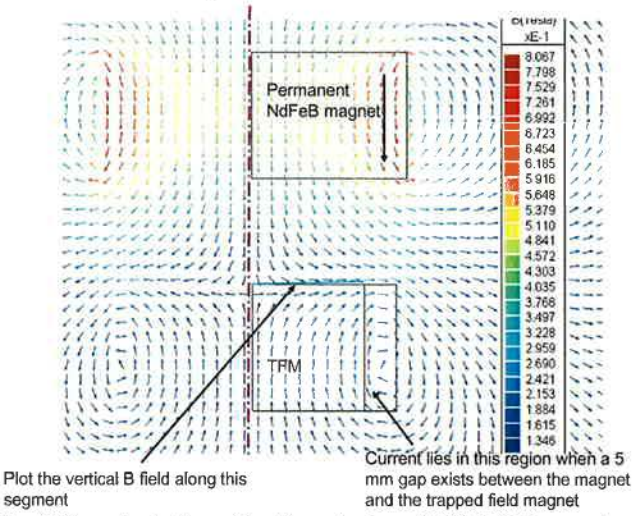

Fig. 5 Magnetic field resulting from placing a 0.5 T NdFeB magnet over a zero field cooled 14 mm diameter TFM.

There are four ways to approach this force calculation.

1. Discretize the complete TFM. Assign current density $J_c = 2.198 \cdot 10^8$ A/m^2 to every sub block to minimize flux linkage within the puck.
2. Assign a current density of J_c to the region from some unknown radius r to the outer radius of the puck. Choose that radius to minimize the net flux penetrating the puck.
3. Break the puck into multiple sub-conductors; assign a zero voltage excitation to the sub-conductors.
4. Repeat step 3, but after each calculation, adjust the current density to J_c for all regions with induced current exceeding J_c.

Method 1 is quite time consuming. Methods 2 and 3 were executed with some success. For method 2, the vertical B field along the upper edge of the TFM puck (annotated in Fig. 5) was computed. A variable metric approach was used to select the current density fill radius so that the flux penetrating the puck was minimized.

Fig. 5 shows what the vector B field looks like as the current density in the TFM builds from the outer radius in to minimize flux linkage.

Fig. 6 shows a comparison of these techniques. Positioning the placement of J_c to minimize flux linkage yields the best fit to the measured data. Method 3 was attempted with 12 and 24 sub-blocks assigned with voltage zero and analyzed with ac. The current density induced in the outer radius blocks exceeded J_c at zero gap distance. The zero gap force drops to 19.2 N when the voltage requirement is dropped for those sub-blocks and substituted with a fixed current density of J_c.

VI. Conclusion

The most expeditious way to compute fields and forces is to break the TFM puck into voltage fed sub-regions. The current is adjusted to ensure $J<J_c$. The problem is worked at a frequency consistent with flux penetration prior to cooling. J_c may need adjustment depending on temperature and B field.

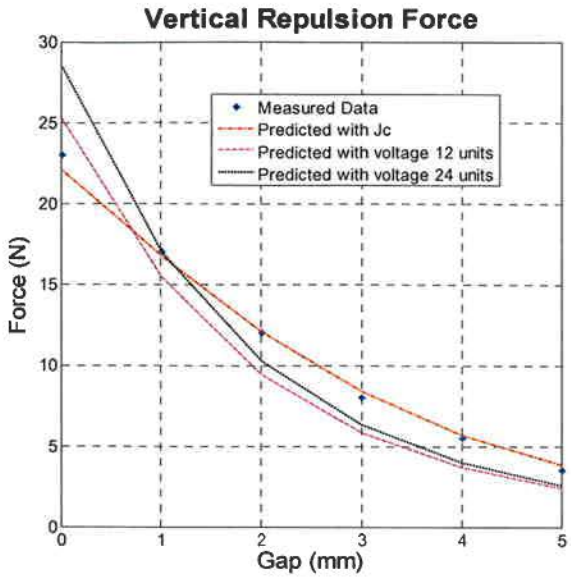

Fig. 6 Force of a NdFeB magnet on a 14 mm diameter TFM magnet at 77°K.

References

[1] G. Fuchs, P. Schätzle, G. Krabbes, S. Grub, P. Verges, K.H. Müller, J. Fink, and L. Schultz, "Trapped magnetic fields larger than 14 T in bulk $YBa_2Cu_3O_{7x}$, Appl. Phy. Lett., vol. 76, no. 15, April 2000, pp. 2107-09.

[2] M. Tomita and M. Murakami, "High temperature superconductor bulk magnets that can trap magnetic fields of over 17 T at 29K", Nature, vol. 421, Jan. 30, 2003, pp. 517-520.

[3] Roy Weinstein, Ravi Sawh, and Alan Crapo, "An experimental generator using high temperature superconducting quasi-permanent magnets", *IEEE Trans. App. Sup.*, vol. 5, no.2, June 1995, pp. 441-444.

[4] Kent R. Davey, "Designing high temperature superconductor magnets," IEEE *Trans. on Magnetics*, Vol. 6, No. 4, pp. 160-166, Dec. 1996.

[5] E. Portabella, R. Palka, H. May, and W.R. Canders, "Static and dynamic model of a HTSC axial bearing", *7th International Symp. On Magnetic Bearings*, Zurich Switzerland, 23-25 August, 2000.

[6] M. Qiu, Z. Xu, Z. H. Yao, D. Xia, L. Z. Lin, G. M. Zhang, L. Xiao, H. T. Ren, Y. L. Jiao, M. H. Zheng, *IEEE Trans. Applied Superconductivity*, Vol. 15, No. 2, part 2, June 2005, pp. 1480-1483.

[7] H. Matsuzaki, I. Ohtani, Y. Kimura, M. Izumi, T. Ida, H. Sugimoto, M.Miki, and M. Kitano, IEEE Transactions on Applied Superconductivity, 15(2005), pp. 2222-2225.

[8] Ryszard Palka, "Modeling of high temperature superconductors and their applications", *International Compumag Society Newsletter*, vol. 12, no. 3, ISSN 1026-0854, Nov. 1, 2005, pp. 3-12.

[9] W. R. Cendes, H. May, R. Palka, "Identification of the current density distribution of monolithic superconductors", International Symposium on Theoretical Electrical Engineering, Palermo, Italy, June 9-11, 1997.

[10] P. E. Gill, W. Murray, and M. H. Wright, Practical Optimization, London, Academic Press, 1981.

[11] William R. Smythe, Static and Dynamic Electricity, Hemisphere Publishing, New York, 1989, pp. 290-291.

[12] M. Abramowitz and I. Stegun, Handbook of Mathematical Functions, Dover, New York, 1970, p. 917.

[13] C.P. Bean, "Magnetization of Hard Superconductors", Physical Review Letters, vol. 8, no. 6, March 15, 1962, pp. 250-253.

[14] Y.B. Kim, C.F. Hempstead, and A.R. Strnad, "Magnetization and Critical Supercurrents", Physical Review, vol. 129, no. 2, Jan. 1963, pp. 528-536.

[15] I. Chen, J. Liu, R. Weinstein, and K. Lau, "Characterization of YBCO including critical current density Jc by trapped magnetic field", *J. Appl. Phy.*, vol. 72, no. 3, Aug. 1992, pp. 1013-1020.

[16] H. Matsuzaki, I. Ohtani, Y. Kimura, M. Izumi, T. Ida, H. Sugimoto, M.Miki, and M. Kitano, IEEE Transactions on Applied Superconductivity, 15(2005), pp. 2222-2225.